Fatigue Life Prediction of Different Joint Designs for Friction Welding of 1050 Mild Steel and 1050 Aluminum

A. Chennakesava Reddy

Abstract— The purpose of this work was to assess vee-joint, square joint and plain joint, used for joining of dissimilar1050 mild steel and 1050 aluminum alloy materials by continuous drive friction welding. Three joints were evaluated for their strength, hardness, fatigue life, heat affected zone and metal flow across the weld joints. This article dealt with complete failure data (all samples were tested until they failed). The vee-joint found to be the superior alternative for the dissimilar materials in continuous drive friction welding.

Index Terms— joint, 1050mild steel, 1050 aluminum alloy, fatigue, friction welding.

1 INTRODUCTION

FRICTION welding is a solid-state welding process that allows material combinations to be joined than with any other welding process. In continuous drive friction welding, one of the workpieces is attached to a motor driven unit while the other is restrained from rotation as showed in figure 1a. The motor driven workpiece is rotated at a predetermined constant speed. The workpieces to be welded are forced together and then a friction force is applied as shown in figure 1b. Heat is generated because of friction between the welding surfaces. This is continued for a predetermined time as showed in figure 1c. The rotating workpiece is halted by the application of a braking force. The friction force is preserved or increased for a predetermined time after the rotation is ceased (figure 1d). Figyre1also illustrates the variation of welding speed, friction force and forging force with time during various stages of the friction welding process.

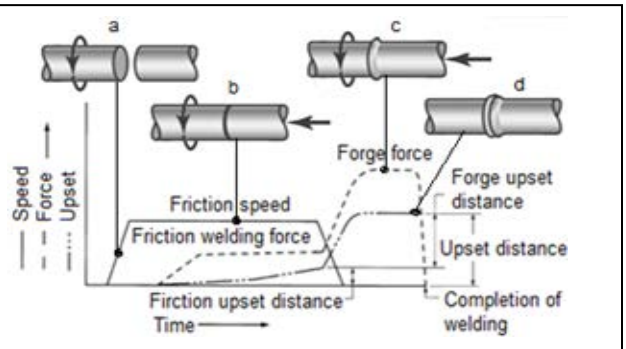

Fig. 1. Friction welding.

With friction welding, joints are possible between not only two solid materials or two hollow parts, but also solid material/hollow part combinations can be reliably welded. However, the shape of a fusion zone in friction welding is dependent the force applied and the rotational speed. If the applied force is too high or the rotational speed is too low, the fusion zone at the centre of the joint will be narrow as showed in figure 2a. On the other hand, if the applied force is too low or the rotational speed is too high, the fusion zone at the centre of the joint will be wider as showed in figure 2b. In both the cases, the result is poor weld joint strength.

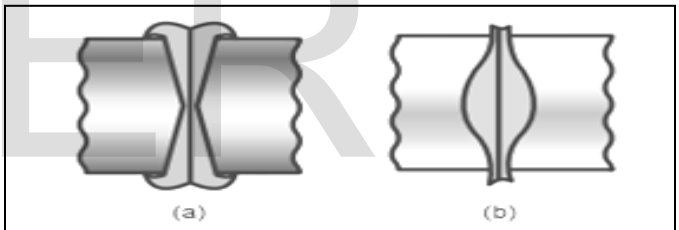

Fig. 2. Effect of force and rotational speed in friction welding.

The foremost difference between the welding of similar materials and that of dissimilar materials is that the axial movement is unequal in the latter case whilst the similar materials experience equal movement along the common axis. This problem arises not only from the different coefficients of thermal expansion, but also from the distinct hardness values of the dissimilar materials to be joined. The Microstructural evolution of the interface of medium carbon steel/austenitic stainless steel depends on thermo-chemical interactions between the two materials [1].Joint and edge preparation is very important to produce distortion free welds. The solid-state diffusion is slow in the wider joints [2].The intermetallic compounds can change the micro hardness near the joint interface of dissimilar metals [3].

Hence, friction welding of dissimilar metals needs to be eased by ensuring that both the workpieces deform similarly. In this context, the objective of the present work is to modify the joint design for the joining interface of 1050 aluminum/1050 mild steel. The fatigue life is determined for all the joints fabricated by the friction welding.

- *A. Chennakesava Reddy, Professor in mechanical engineering, JNT University, Hyderabad, India, PH-+91 9440568776. E-mail: acreddy@jntuh.ac.in*

2 MATERIALS AND METHODS

The materials used in this work are mild steel and 1050 aluminum alloy. These materials were welded with three types of proposed joints. The mild steel and austenite stainless steel cylindrical bars of 25mm diameter were first cut to the length of about 300mm on an automatic hacksaw machine. The designs of three weld joints namely vee joint, square joint and plain joint are shown in figure 3.

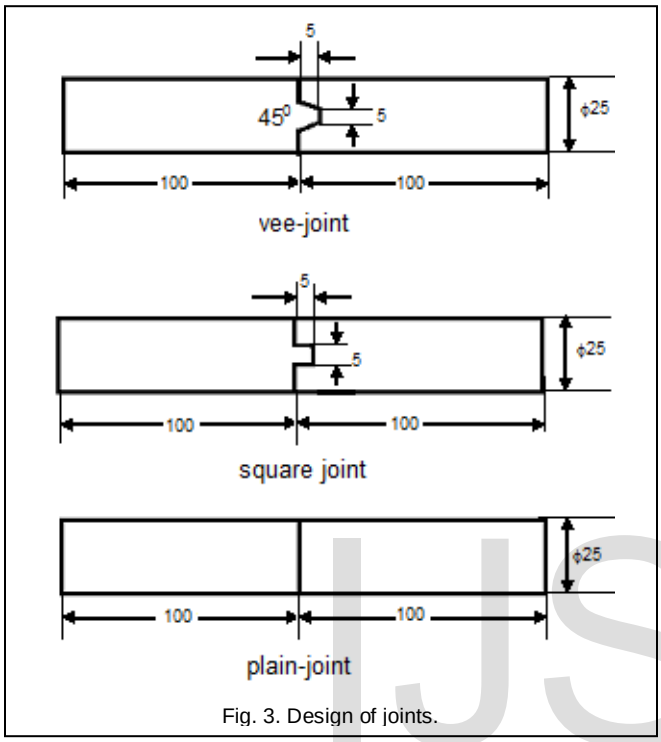

Fig. 3. Design of joints.

The specimens were machined as per the dimensions of the designed joints (Fig. 3) on a lathe machine. After machining operation, these specimens were thoroughly cleaned, washed with distilled water, and finally dried. Friction welding was performed using a pressure servo-controlled brake type machine. The mild steel workpiece was held on the motor driven unit and the 1050 aluminum workpiece was fixed in the static holding device. The machine then was scheduled for its rotational speed as per the intended value and started welding process. Axial movement was then given to 1050 aluminum workpiece till both the workpieces come into contact with each other. The welding parameters were rotational speed (1500 rpm), friction pressure (120 MPa), friction time (10 sec), upset pressure (180 MPa) and upset time (25sec). The welded workpiece was then withdrawn from the machine. A flash, which was built during the welding process, was machined by holding the workpiece in the chuck of the lathe machine. The microstructure of joints was investigated using an optical microscope. The welded specimens were tested for tensile strength on a universal testing machine (UTM). The increase in hardness in the vicinity of the joint was determined in accordance with a Rockwell hardness tester to find the heat affected zone (HAZ). The effect of joint design on HAZ and material flow was also assessed through microstructures.

For the fatigue test, the applied stresses were axial (tension-compression) with low cycle completely reversed constant amplitude where the alternating stress varied from a maximum tensile stress to a minimum compressive stress of equal magnitude. Ten smooth specimens of each joint were tested under strain controlled conditions in order to evaluate the survival of joints. Geometry and dimensions (ASTM E606) of the fatigue test specimens are shown in figure 4. After machining the specimens to the desired geometry, the specimen surfaces were mechanically polished. The experiments were carried out in a close-loop servo hydraulic test machine with 100 kN load capacity. A sinusoidal waveform was used as a command signal. The fatigue tests were conducted with constant strain amplitudes in atmospheric air conditions. The flashless specimens were cyclic-loaded under strain control with symmetrical push-pull loading, with a nominal strain ratio of 0.1, maximum load of 8KN, a minimum load of -4KN and frequency 10Hz.

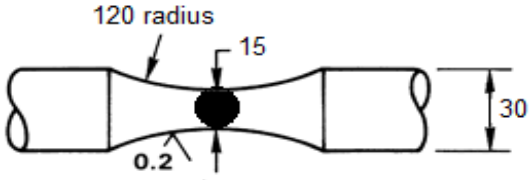

Fig. 4. Specimen of fatigue test (all dimensions are in mm).

3 ESTIMATION OF WEIBULL PARAMETERS

Weibull analysis is a method for modeling data sets containing values greater than zero, such as failure data. Weibull analysis can make predictions about the life of a weld joint. The Weibull cumulative distribution function can be transformed so that it is provided in the form of a straight line ($y=mx+c$). To compute Weibull cumulative distribution the following formulae are used:

$$F(x) = 1 - \exp\left(-(x/a)^{\beta}\right) \quad (1)$$

$$\ln(1-F(x)) = -(x/a)^{\beta}$$

$$\ln(1/1-F(x)) = (x/a)^{\beta}$$

$$\ln\left[\ln(1/(1-F(x)))\right] = \beta \ln(x/a)$$

$$\ln\left[\ln(1/1-F(x))\right] = \beta \ln x - \beta \ln \alpha \quad (2)$$

where β is the shape parameter α is the scale parameter and x is the maximum fatigue cycles.

Comparing Eq.(2) with the simple equation of a line, we see that the left side of Eq.(2) corresponds to Y, $\ln x$ corresponds to X, β corresponds to m, and $-\beta \ln \alpha$ corresponds to c. When the linear regression is performed, the estimate for parameter β comes directly from the slope of the line. The estimate of the parameter α must be calculated as follows:

Comparing Eq.(2) with the simple equation for a line, we see that the left side of Eq.(2) corresponds to Y, $\ln x$ corresponds to X, β corresponds to m, and $-\beta \ln \alpha$ corresponds to c. When the linear regression is performed, the estimate for the parameter β comes directly from the slope of the line. The estimate of the parameter α must be calculated as follows:

$$\alpha = \exp(-c/\beta) \quad (3)$$

4 Results and Discussion

The microstructure of mild steel (base metal) is shown in figure 5a. The white areas reveal ferrite and dark areas represent pearlite in the 1050 mild steel. The microstructure of 1050 aluminum (base metal) is shown in figure 5b. The second phase particles are aligned with the rolling direction forming colonies of clusters. The discrepancy in grain size is closely related to the concentration gradients developed during casting and amount of subsequent cold rolling operations.

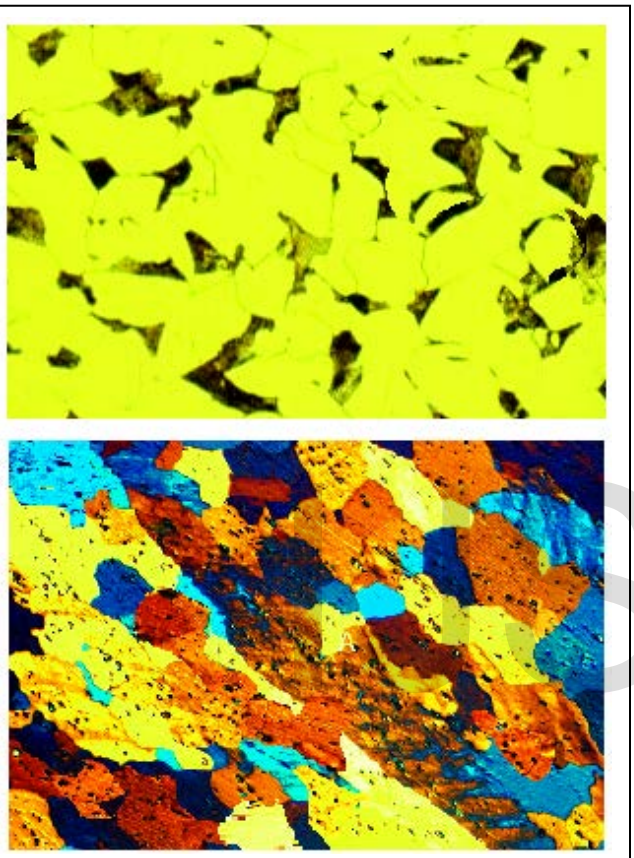

Fig. 5. Microstructures of base metals (a) mild steel and (b) 1050 aluminum alloy.

4.1 Joint Strengths

The surface areas of vee-joint, square joint and plain-joint are A_v, A_s and A_p respectively. Figure 6 shows the ultimate tensile strength of different weld joints. Ultimate tensile strength of vee-joint is greater than of square-joint and plain-joint. The square-joint is under a greater area of contact than vee-joint and plain-joint ($A_s > A_v > A_p$). However, the distribution of upset pressure is not uniform in the square-joint during friction welding due to its profile resulting in poor weld joint. The contact area of vee-joint is greater than of plain-joint ($A_v > A_p$) and smaller than that of square-joint ($A_v < A_s$). In vee-joint, the upset pressure distribution is uniform owing to its profile resulting in good weld joint.

4.2 Heat Affected Zone

Heat affected zone (HAZ) is that portion of the base metal, where mechanical properties and microstructures are modified by the heat of welding. HAZ is often determined by the response of the weld joint to the hardness or etching effect tests. Friction welding produces very limited and narrow HAZ.

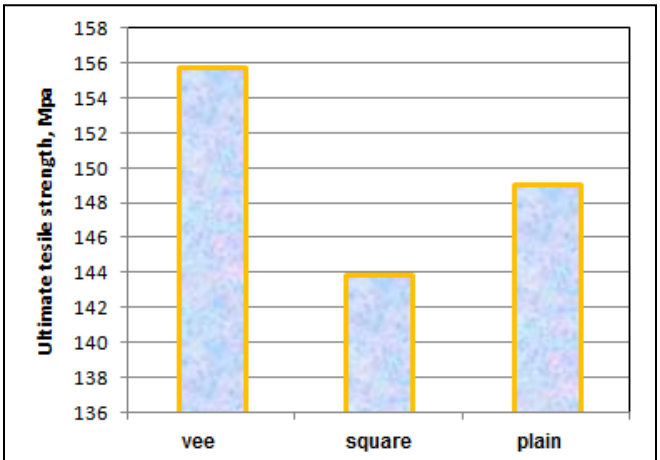

Fig. 6. Ultimate tensile strength of joints.

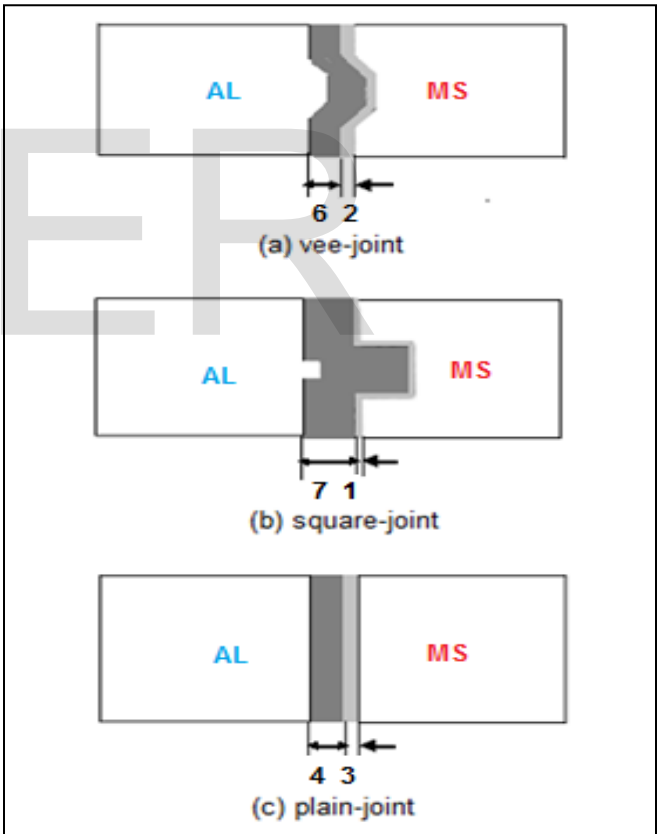

Fig. 7. Heat affected zones (HAZ) in different joints.

Figure 7a shows HAZ width from the center line of vee-joint is 6mm for the aluminum and 2mm for the mild steel. Figure 7b shows that the HAZ width is 7mm on the aluminum side from the center line of square-joint and it is 1mm on the mild steel side. HAZ width is 4mm on the aluminum side from the center line of plane-joint and it is 3mm on the mild steel side as showed in Figure 7c. Figure 8 shows the hardness

distribution for the weld joints. The hardness profile across the weld joint shows a sharp peak in the vicinity of weld interface that may affect the properties of the weld joint. The hardness distribution was proved to be higher in the square-joint as compared to the other two joints. Hardness distribution on the mild steel is greater than of the aluminum side, because the fusion zone is in the aluminum side for all the joints.

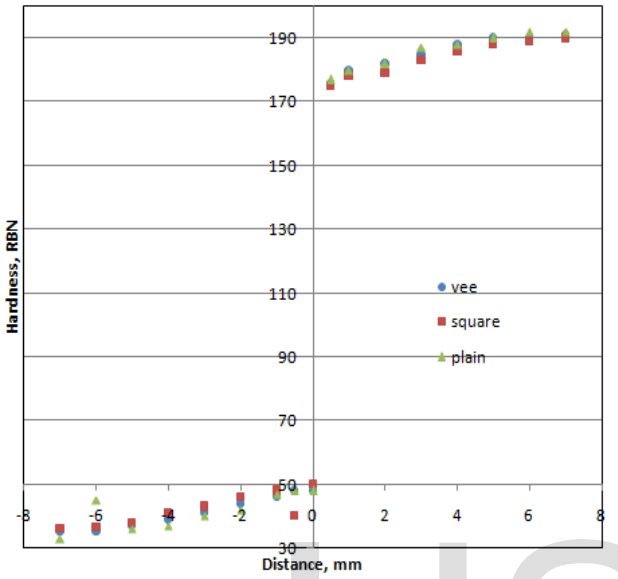

Fig. 8. Hardness distributions across the joints

4.2 Microstructural Evaluation of Weld Joints

Figure 9a reveals the microstructure and material flow of friction welded vee-joint. It shows a fine metal flow and a good mixture of mild steel and aluminum materials at the interface. Plasticized aluminum slides over the slant surfaces of vee-joint and formed flash on the periphery of specimens. The fine grain size structure was obtained at HAZ and weld zones. After cooling and applying the subsequent pressure, the process of recrystallization and growth took place that resulted in a fine grain structure. HAZ was raised to 6mm in the aluminum. According to the Hall-Petch equation, material strength depends on the grain size, and the smaller grains produce higher strengths. Figure 9b exposes the microstructure of friction welded square-joint. It shows no flow of material and there is the absence of mixing of two materials. The heat affected zone of aluminum reveals fine grained structure. The fusion zone reveals a coarse grain structure. The microstructure on the austenite steel side has not much affected except at the interface because HAZ is extended to 1mm only, whereas the same is extended to 7mm on the aluminum side. Very interestingly the microstructure reveals the radial distribution of grains in the aluminum part circumferential distribution of grains in the mild steel at the interface. This might be due to conduction of the heat due to friction in the radial direction in the aluminum.

Figure 9c reveals the microstructure of friction welded plain-joint. In HAZ, the transition is observed from coarse grain pattern of ferrite-pearlite to partially crystallized ferrite-pearlite structure in the mild steel at the interface. The coarse grain structure is observed in the aluminum. Microphotograph shows that aluminum is greatly deformed with grains elongated and refined near the weld interface.

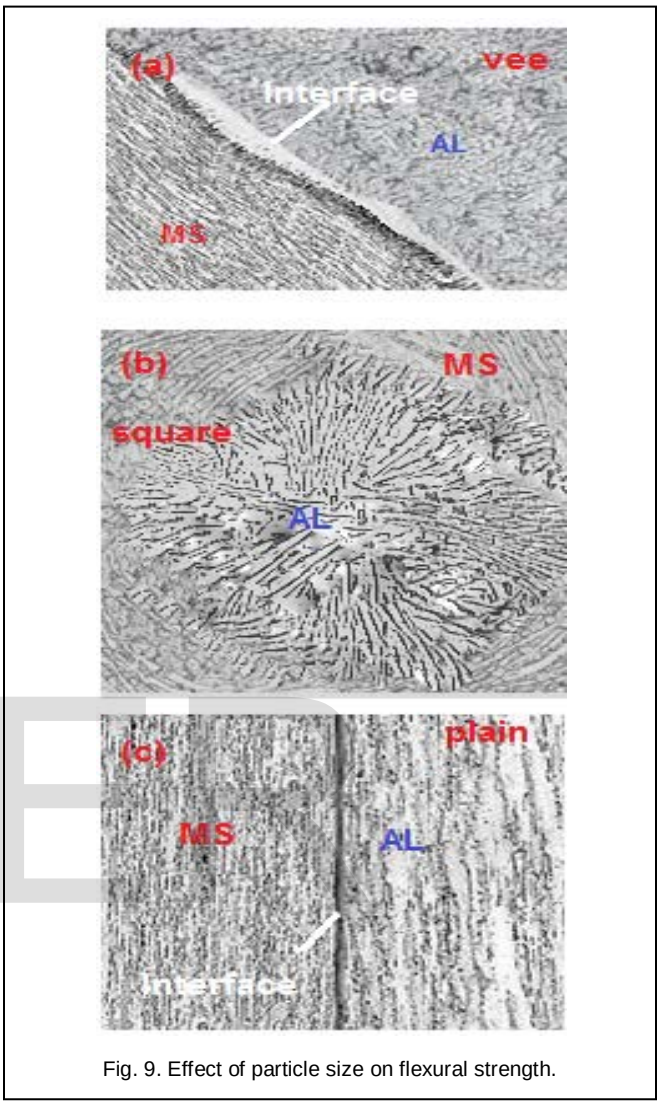

Fig. 9. Effect of particle size on flexural strength.

Another interesting welding was carried out as shown in figure 10. This square joint was very pathetic having very low strength and there were burning spots in the mild steel due to rubbing action against the aluminum. It was also observed that there was a melt of aluminum at some spots at the interface.

4.3 Weibull Criteria

The Weibull shape parameterβ indicates whether the failure rate is increasing, constant or decreasing. A β <1.0 indicates that the product has a decreasing failure rate. This scenario is typical of "infant mortality" and indicates that the joint is failing during its "burn-in" period. A β=1.0 indicates a constant failure rate. A β >1.0 indicates an increasing failure rate. This is characterized by products that are worn out. Three joint designs: vee-joint, square-joint, and plain-joint have β values much higher than 1.0 as seen in Fig. 15. The joints fail due to fatigue, i.e., they wear out. The straight line equation for vee-joint was obtained as:

$$y = 51.62x - 410.8 \quad (4)$$

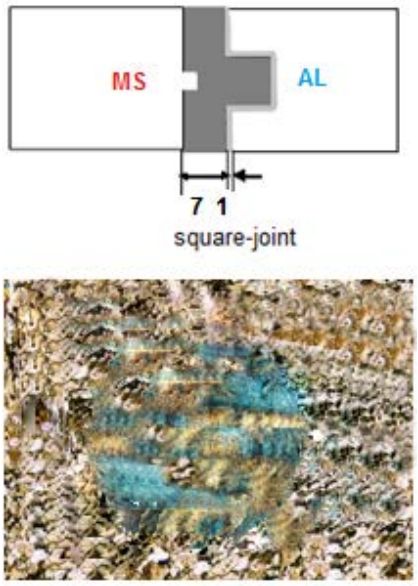

Fig. 10. Mild steel inside aluminum outside square joint.

The straight line equation for plain-joint was computed as:

$$y = 93.772\,x - 700.2 \quad (5)$$

The straight line equation for square-joint was determined as:

$$y = 85.34x - 656.7 \quad (6)$$

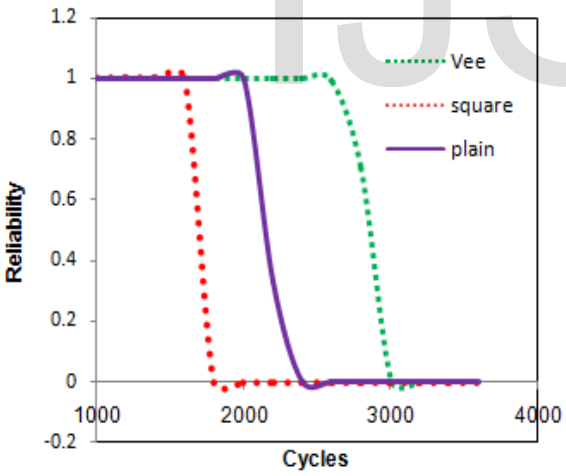

Fig. 11. Reliability of joints.

The Weibull characteristic life measures as the scale in the distribution of data. It so happens that α equals the number of cycles of which 63.2 percent of the joint has failed. In other words, for a Weibull distribution R (= 0.368), regardless of the value ofβ. Survival fatigue cycles for about 37 percent of vee-joints, plane joints, and square joints are respectively 2859, 2197 and 1749.

5 Conclusion

Within the framework of the design considerations and experimental conditions used and the aims of this investigation, the following conclusions can be drawn:

- The vee-joint welds have resulted in higher tensile strength than square and plain joint welds.
- The metal flow is also good in the vee joint weld.
- This article proves that alternative weld joints to plain joint are feasible for the friction welding process.
- At 2500 cycles, the survivability of vee-joint welds was 99 percent, whereas the survivability of plain-joint and square joint welds were totally failed.

Acknowledgment

The authors wish to thank University Grants Commission (UGC), New Delhi, India for financial assisting this project.

References

[1] M. Sahin, and H.E. Akata, "An experimental study on friction welding of medium carbon and austenitic stainless-steel components", Indust. Lubri. Tribol., vol. 2004, vol.56, pp.122-129.

[2] A. Chennakesava Reddy, A. Ravaivarma, and V. Thirupathi Reddy, in Proc. National Welding Seminar, IIT-Madras, 2002, pp.51-55.

[3] W. Li and F. Wang, "Modeling of continuous drive friction welding of mild steel", Mater. Sci. Eng. A; 2011 , vol. 528, pp.5921-5926.